Electronic Supplementary Materials

Plasma Promotes Dry Reforming Reaction of CH_4 and CO_2 at Room Temperature with Highly Dispersed NiO/γ-Al_2O_3 Catalyst

Shan-Shan Lin [1,2], Peng-Rui Li [1,2], Hui-Bo Jiang [1,2], Jian-Feng Diao [2,*], Zhong-Ning Xu,[2,*] and Guo-Cong Guo [2]

[1] College of Chemical Engineering, Fuzhou University, Fuzhou 350116, China

[2] State Key Laboratory of Structural Chemistry, Fujian Institute of Research on the Structure of Matter, Chinese Academy of Sciences, Fuzhou 350002, China

* Correspondence: diaojianfeng@fjirsm.ac.cn (J.-F.D.); znxu@fjirsm.ac.cn (Z.-N.X.)

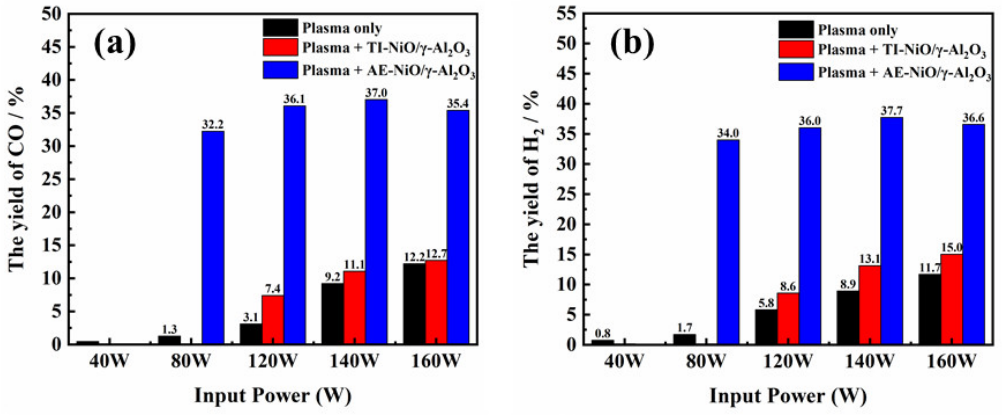

Figure S1. Effect of different reaction modes on the performance of the plasma dry reforming reaction: (a) yield of CO, (b) yield of H_2. (CO_2/CH_4 = 1 : 1, total feed flow rate 20 mL/min, 600 mg catalyst, room temperature and ambient pressure).

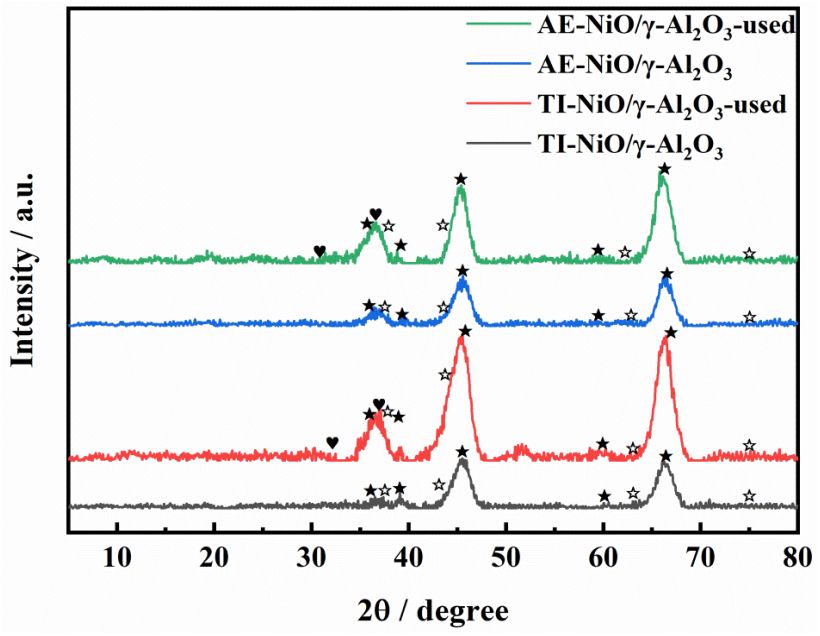

Figure S2. PXRD pattens of AE-Ni/γ-Al_2O_3-used, TI-Ni/γ-Al_2O_3-used (☆NiO, ★γ-Al_2O_3, ❤ $NiAl_2O_4$).

It can be seen from the Figure S2 that the diffraction peaks of AE-Ni/γ-Al_2O_3-used and TI-Ni/γ-Al_2O_3-used around 37 ° were significantly enhanced, but no obvious carbon diffraction peak was found, which may be attributed to the formation of $NiAl_2O_4$ (2θ = 31.406 °, 2θ = 31.406 °, PDF # 10-0339). That also means that during the reaction, NiO interacted with the support γ-Al_2O_3 to form a $NiAl_2O_4$ spinel. In addition, no obvious diffraction peaks of Ni or NiO were observed, which proved that NiO was not sintered or cluster after the reaction.

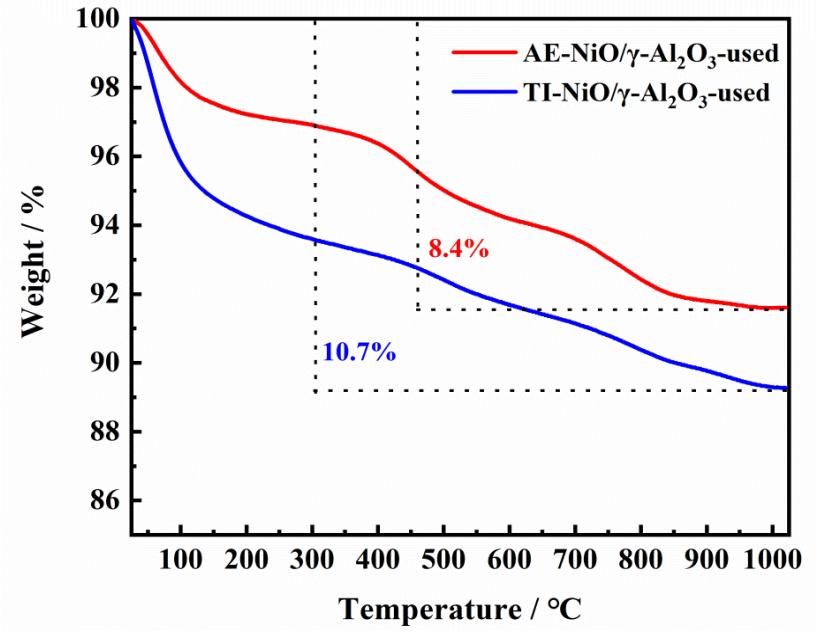

Figure S3. TG results of AE-Ni/γ-Al_2O_3-used and TI-Ni/γ-Al_2O_3-used.

Figure S3 shows the TG results of AE-Ni/γ-Al_2O_3-used and TI-Ni/γ-Al_2O_3-used. Obviously, the loss of AE-Ni/γ-Al_2O_3-used is less than TI-Ni/γ-Al_2O_3-used. By combining the EDX results in Figure S4, it can be obtained that carbon is formed on the catalyst after the reaction. As shown in

Figure S3, the weight loss of AE-Ni/γ-Al_2O_3-used is less than the weight loss of TI-Ni/γ-Al_2O_3-used, indicating that the ability to resist carbon deposition of AE-Ni/γ-Al_2O_3 is higher than TI-Ni/γ-Al_2O_3.

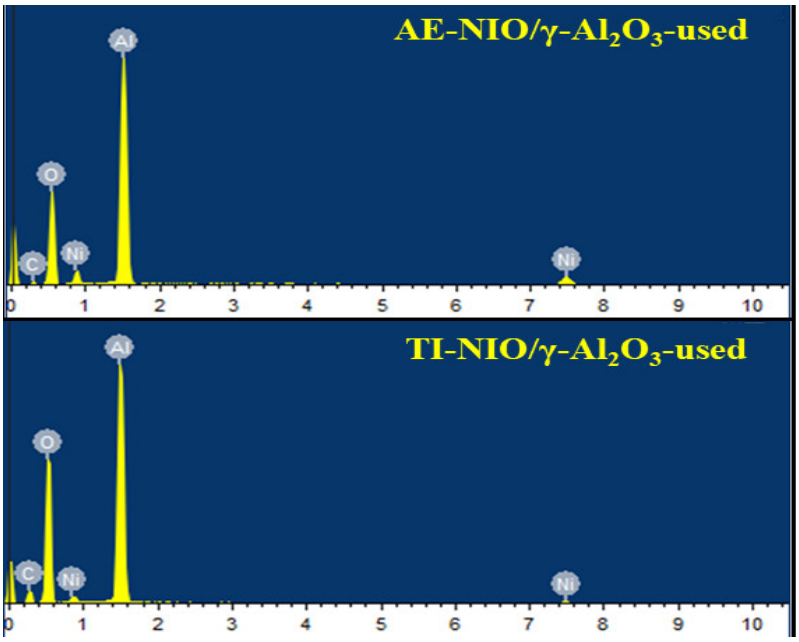

Figure S4. EDX results of AE-NiO/γ-Al_2O_3-used and TI-NiO/γ-Al_2O_3-used.

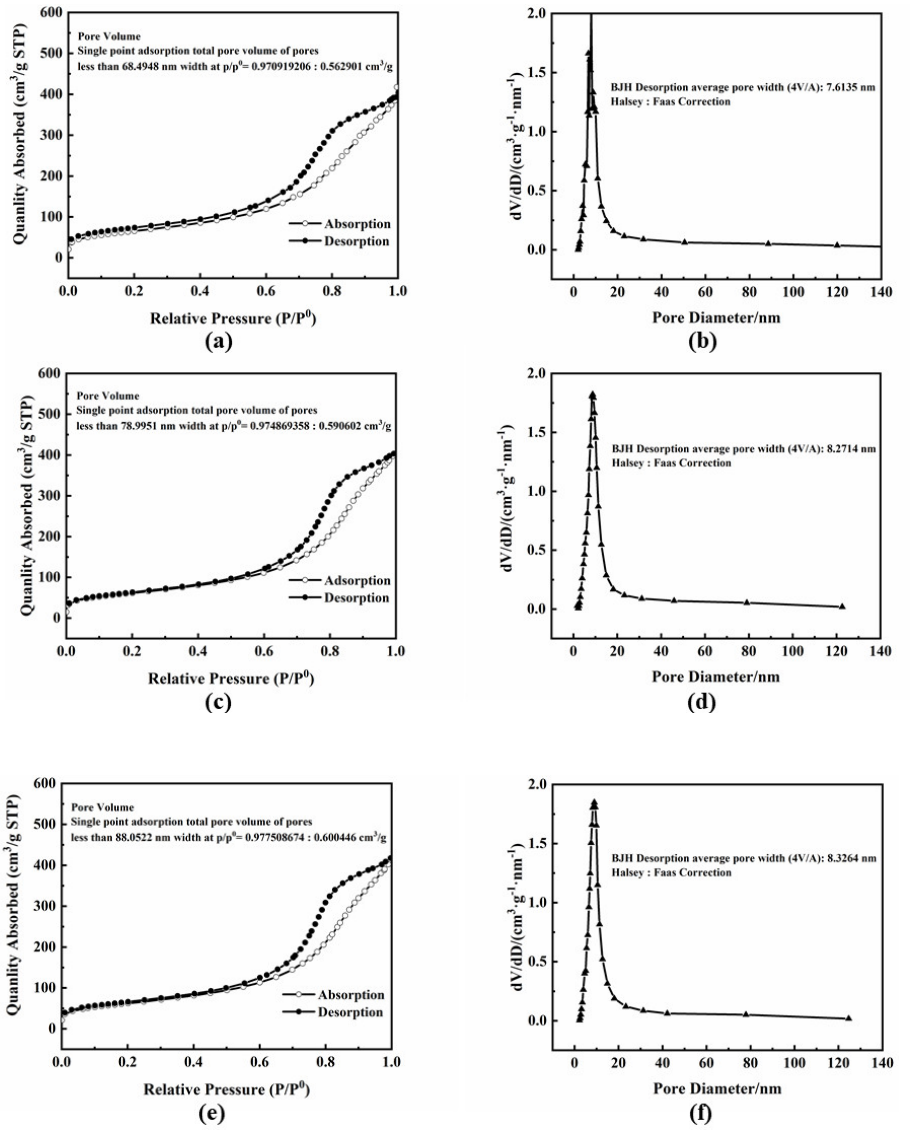

Figure S5. (a) Nitrongen adsorption isotherms of γ-Al_2O_3, (b) BJH desorption average pore size distribution of γ-Al_2O_3, (c) Nitrongen adsorption isotherms of AE-NiO/γ-Al_2O_3, (d) BJH desorption average pore size distribution of AE-NiO/γ-Al_2O_3, (e) Nitrongen adsorption isotherms of TI-NiO/γ-Al_2O_3, (f) BJH desorption average pore size distribution of TI-NiO/γ-Al_2O_3.

Table S1. Input Power, Output Power (Discharge Power) and Efficiency.

Input Power(W)	Output Power(W)	Efficiency(η, %)
40	36.4	91.1
80	64.7	80.8
120	92.7	77.3
140	132.1	94.4
160	147.6	92.2

Table S1 lists the input power and discharge power calculated by the Lissa-jous graphic method. The discharge efficiency is calculated by $Efficiency(\eta) = \frac{Output\ Power}{Input\ Power} \times 100\%$.